Pulsed-power-driven cylindrical liner implosions of laser preheated fuel magnetized with an axial field[a)]

S. A. Slutz,[b)] M. C. Herrmann, R. A. Vesey, A. B. Sefkow, D. B. Sinars, D. C. Rovang, K. J. Peterson, and M. E. Cuneo
Sandia National Laboratories, Albuquerque, New Mexico 87185, USA

(Received 20 November 2009; accepted 3 February 2010; published online 12 March 2010)

The radial convergence required to reach fusion conditions is considerably higher for cylindrical than for spherical implosions since the volume is proportional to r^2 versus r^3, respectively. Fuel magnetization and preheat significantly lowers the required radial convergence enabling cylindrical implosions to become an attractive path toward generating fusion conditions. Numerical simulations are presented indicating that significant fusion yields may be obtained by pulsed-power-driven implosions of cylindrical metal liners onto magnetized (>10 T) and preheated (100–500 eV) deuterium-tritium (DT) fuel. Yields exceeding 100 kJ could be possible on Z at 25 MA, while yields exceeding 50 MJ could be possible with a more advanced pulsed power machine delivering 60 MA. These implosions occur on a much shorter time scale than previously proposed implosions, about 100 ns as compared to about 10 μs for magnetic target fusion (MTF) [I. R. Lindemuth and R. C. Kirkpatrick, Nucl. Fusion **23**, 263 (1983)]. Consequently the optimal initial fuel density (1–5 mg/cc) is considerably higher than for MTF ($\sim$1 μg/cc). Thus the final fuel density is high enough to axially trap most of the α-particles for cylinders of approximately 1 cm in length with a purely axial magnetic field, i.e., no closed field configuration is required for ignition. According to the simulations, an initial axial magnetic field is partially frozen into the highly conducting preheated fuel and is compressed to more than 100 MG. This final field is strong enough to inhibit both electron thermal conduction and the escape of α-particles in the radial direction. Analytical and numerical calculations indicate that the DT can be heated to 200–500 eV with 5–10 kJ of green laser light, which could be provided by the Z-Beamlet laser. The magneto-Rayleigh-Taylor (MRT) instability poses the greatest threat to this approach to fusion. Two-dimensional Lasnex simulations indicate that the liner walls must have a substantial initial thickness (10–20% of the radius) so that they maintain integrity throughout the implosion. The Z and Z-Beamlet experiments are now being planned to test the various components of this concept, e.g., the laser heating of the fuel and the robustness of liner implosions to the MRT instability. © *2010 American Institute of Physics*.
[doi:10.1063/1.3333505]

I. INTRODUCTION

Pulse-power-driven z pinches convert their radial kinetic energy to x rays upon stagnation. High ($\sim$15%) overall efficiency (wall plug to x-ray radiation) has been demonstrated.[1] These x rays could be used to drive inertial confinement fusion (ICF) capsules. Numerical designs[2] indicate that approximately 18 MJ of x rays are needed to ignite an ICF capsule with a yield of about 500 MJ. The capsule only absorbs about 1.2 MJ of the x rays, while the hohlraum walls absorb the rest. Furthermore, only about 15% of the energy absorbed by the capsule contributes to the kinetic energy of the implosion. Thus only a small fraction ($\sim$1%) of the x-ray energy is converted into kinetic energy of the imploding ICF fuel. Clearly a much larger amount of implosion kinetic energy would be available if the two-step conversion process (kinetic to radiation and then radiation to kinetic) could be avoided.

In this paper we consider the direct implosion of cylindrical liners to obtain fusion conditions using the magnetic pressure generated by the current produced by pulsed power machines such as Z. The natural geometry of magnetically imploded systems is cylindrical, which increases the convergence required to reach fusion conditions because the volume scales with the fuel radius squared, as compared to the fuel radius cubed for spherical implosions. As we shall show, preheating and magnetizing the fuel can significantly reduce the required radial convergence.

Although it was recognized as early as 1949 that a magnetic field could significantly reduce electron thermal conductivity,[3] it was several years after the seminal paper[4] proposing ICF that magnetized fuel was proposed[5] and the first experiments demonstrating that a magnetic field could improve ICF yields were performed.[6] An intense relativistic electron beam was used to drive capsule implosions in these experiments. Due to the long range of the electrons, the specific energy deposition rate was low and the implosions were slow. A portion of the electron beam current was used to magnetize and preheat the fuel. The subsequent reduction in the electron thermal conductivity was enough to allow the fuel to reach temperatures high enough to generate a measurable number ($>10^6$) of thermonuclear fusion neutrons. In

[a)]Paper JI2 6, Bull. Am. Phys. Soc. **54**, 136 (2009).
[b)]Invited speaker.

 © 2010 American Institute of Physics

Downloaded 18 Jan 2011 to 134.253.26.11. Redistribution subject to AIP license or copyright; see http://pop.aip.org/about/rights_and_permissions

contrast, no neutrons could be measured for implosions without fuel magnetization. High yield designs were later proposed for charged-particle beam capsules based on fuel magnetization,[7] but no further experiments were performed.

Lindemuth and Kirkpatrick[8] explored the parameter space for magnetized fuel ICF capsules. Their model calculations showed that significant gain could be obtained for relatively slow implosion velocities (<1 cm/μs) when a magnetic field provided magnetothermal-insulation and the initial fuel densities were low (~ 1 μg/cc). A number of researchers are presently exploring this regime, often referred to as magnetized target fusion[9] (MTF), which lies between magnetic confinement and ICF in parameter space. The primary attraction is that the power required to drive these slow velocity implosions is significantly smaller than required for standard ICF and could offer a low cost approach to fusion.[10] Jones and Mead[11] performed more detailed numerical simulations, which supported the conclusion that a magnetic field could improve volume burn. However, they also showed that a magnetic field inhibited the propagation of a deflagration burn wave into any surrounding fuel. This result suggests that MTF will have gains not much more than about 10. However, in contrast to laser-driven ICF, large gains may not be needed for fusion energy via MTF, due to the high efficiency of pulsed-power drivers and magnetically driven implosions. In addition, gains less than unity could be useful for a hybrid fission/fusion scheme[12] where fusion neutrons are used to burn actinides. It is also possible that higher gains could be possible with some variation in this approach.[13] Even without commercial application, fusion yields with gains greater than unity would be interesting for the study of fusion physics in the laboratory.

Several means to magnetize and preheat fusion fuel have been proposed. One method, first developed in Russia,[14] is MAGO (MAGnitnoye Obzhatiye, or magnetic compression). This approach is based on a two-chamber discharge that generates an inverse z pinch in the first and injects high velocity plasma into the second where this plasma is further ionized and heated by stagnation. This fusion plasma would subsequently be compressed with a magnetically driven liner,[15] which implodes in several microseconds. Another approach has been proposed based on generating a field-reversed plasma configuration[16] (FRC). These configurations, which were originally developed as magnetic confinement fusion systems,[17] can be self-sustaining for tens of microseconds, which is long enough to move them to within a metal liner for subsequent compression.[18] FRCs can have[19] plasma densities of ~ 0.1 μg/cc and temperatures of 250 eV, and are thus suitable for liner compression with implosion times of ~ 10 μs. An interesting feature of FRCs is that the field geometry is believed to remain nearly fixed during an implosion driven by a cylindrical liner. Thus the plasma density and temperature could scale more favorably than for a purely cylindrical implosion.

There is interest in magnetically insulating the fuel within a cylindrical tube heated by an annular heavy ion beam.[20] The physical regime of such implosions would be very similar to what we are proposing. However, there is no accelerator today that can produce the required ion beam with sufficient power and energy to perform fusion experiments on this concept.

It has also been proposed to use laser beams to implode a cylinder containing magnetized fuel.[21] The implosion time of such a system would be less than 10 ns and thus it would be possible to test fuel magnetization at higher densities than is possible with the Z machine. However, laser-driven implosions are not as efficient as magnetically driven implosions and high drive efficiency is required for inertial fusion energy applications when the fusion gain is modest.

In this paper, we present a scenario using pulsed power to drive fast liner implosions (~ 100 ns) with magnetized and preheated fuel. The relatively short implosion time of 100 ns provides some advantages compared to longer implosion times (>10 μs) previous considered for MTF such as the FRC experiments. As we show in the next section, there is a maximum fuel density, which scales inversely with the implosion time. The relatively high fuel density after compression of fast implosions allows the use of a purely axial magnetic field, which only inhibits the radial transport of the α-particles, while the axial transport is simply determined by the α-particle slowing down as in unmagnetized fuel. Thus the minimum axial length of the liner to obtain axial α-particle trapping is determined by the formula $\rho\Delta z \geq 0.5$ g/cm^2, where Δz is the length of the liner. We present numerical simulations indicating that pulsed power liner implosions with optimal yield have final fuel densities of 0.5–1.0 g/cc, which implies that the liner length must be 0.5–1.0 cm. In comparison, a 10 μs liner implosion would require a length of 50–100 cm. Liners of such long extent are difficult to implode due to the large inductance of such loads. Thus a simple axial magnetic field is not suitable for long time scale implosions and more complicated field line configurations are needed such as FRCs or possibly a randomly oriented magnetic field.[22] In addition, the energy required to preheat the fuel scales unfavorably as the implosion time is increased. We find that a modest preheat energy of 6.5 kJ is needed for 100 ns implosions, which could be provided by the Z-Beamlet laser. In contrast, a preheat energy of approximately 650 kJ is required for a 10 μs implosion at optimal fuel density. This would require a very expensive laser or another means to heat the fuel. Thus our proposed approach of using a simple axial magnetic field for fuel magnetization and a laser to preheat the fuel is presently practical only for relatively short implosion times, which are made possible by pulsed power machines such as the Z machine.

In summary, our proposed scenario illustrated in Fig. 1 is as follows. We first magnetize the fuel within a liner by external field coils, as shown in Fig. 1(a). Magnetization must occur on a relatively long time scale >1 ms to allow the magnetic field to diffuse into the liner. The Z machine is then triggered to start the implosion. The Z-Beamlet laser is fired when the inner boundary of the liner starts to move inward. The laser heats a cylindrical region of the fuel with a radius smaller than the initial inner surface of the liner and heats this portion of the fuel to 200–400 eV, which makes the fuel very conductive. The magnetic field is effectively frozen into the fuel and is subsequently compressed as the liner implodes. The magnetic field strength, which is approxi-

Downloaded 18 Jan 2011 to 134.253.26.11. Redistribution subject to AIP license or copyright; see http://pop.aip.org/about/rights_and_permissions

mately proportional to the inverse square of the fuel radius, rises to greater than 100 MG at stagnation. Simulations predict significant fusion yields suggesting this approach could be a path toward economical fusion. However, there are many issues that have to be addressed to determine the commerciality of this scenario and such studies are beyond the scope of this paper. We concentrate on the physics of magnetized liner implosions to study fusion in the laboratory.

II. IGNITION AND GAIN REQUIREMENTS

There are three basic requirements for the ignition and burn of an ICF capsule. The first is that the fuel temperature must be raised above the ideal ignition temperature (~4.3 keV) for a 50:50 mixture of deuterium and tritium (DT). The second requirement is that a sufficient fraction of the fusion energy must be deposited in the fuel for further self-heating. The third is that the fuel must be confined long enough so the fusion yield exceeds the driver energy coupled into the capsule.

A. Implosion physics and preheat requirements

First we consider heating DT plasmas to the ignition temperature. We assume that either a spherical or cylindrical pusher adiabatically compresses a DT gas (PV^{γ}=const with $\gamma=5/3$), which is initially at a temperature θ_0. Note the symbol θ will denote temperature in keV throughout this paper. Since the volume of the fuel is

$$V(t) = V_0\left[\frac{r(t)}{r_0}\right]^g, \tag{1}$$

where V_0 is the initial volume of the fuel, r is the radius of the fuel/pusher interface, the subscript 0 refers to values at $t=0$, and the exponent g is 2 (3) for cylindrical (spherical) convergence, the convergence ratio required to adiabatically compress preheated fuel to the ignition temperature is

$$C_R \equiv \frac{r_0}{r_f} = \left(\frac{\theta_{ig}}{\theta_0}\right)^{3/2g}, \tag{2}$$

which would be a very large number for either geometry unless the fuel is preheated before compression. In a typical ICF capsule, a degree of preheat is provided by a shock wave that is driven into the fuel. Using the relations[23] for a planar strong shock wave in an ideal gas with $\gamma=5/3$, we find the fuel shock temperature is $\theta_s \approx 4.2\times 10^{-4}\ V_p^2$ keV where V_p is the maximum velocity of the pusher (cm/μs). Note that we have ignored the acceleration of the shock due to geometric convergence,[24] which should not introduce large errors since the shock is geometrically accelerated over only a small fraction of the fuel mass near the center. The end of the shock-heating phase occurs when the shock reaches the center of the fuel. At this time, the total volume of the fuel has decreased by approximately 4 and the shell velocity is subsonic relative to the speed of sound within the fuel so we can use Eq. (2) for the subsequent heating with the substitution $\theta_0=\theta_s$. The estimated total convergence required to reach ignition temperature is then

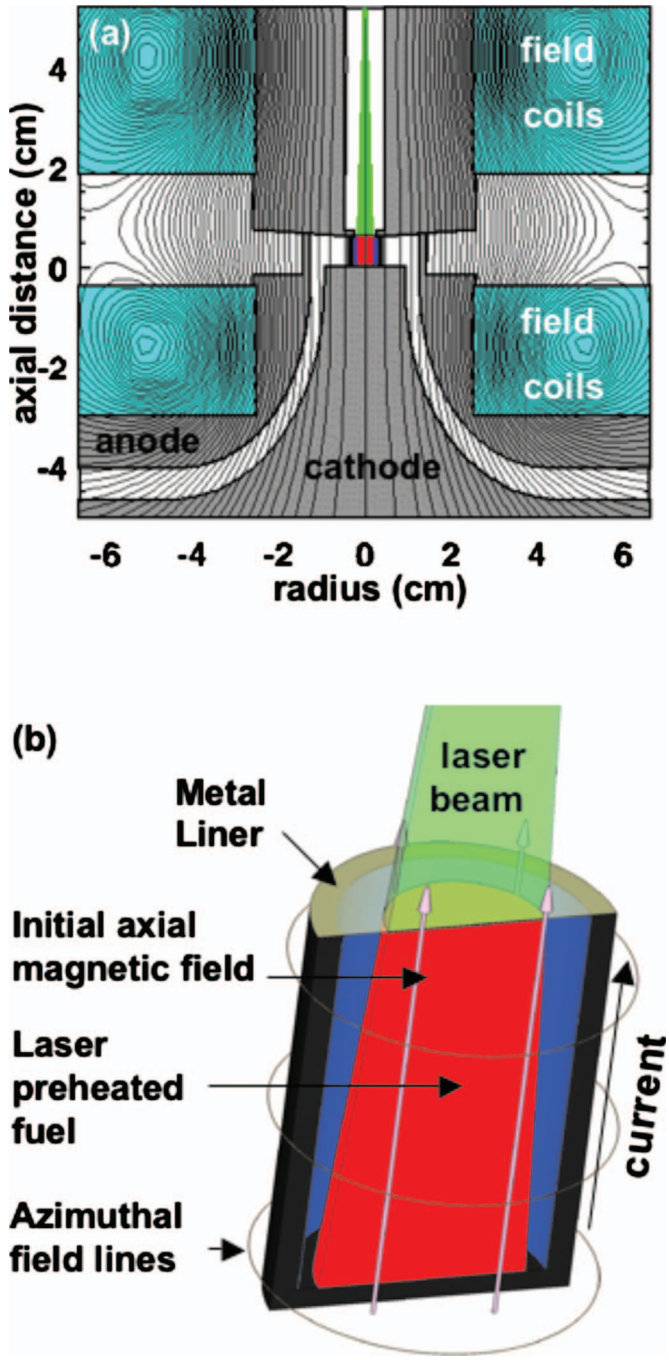

FIG. 1. (Color) Schematic of the MagLIF concept (a) overall geometry including field coils, electrodes, and laser entrance path and (b) a blowup of the liner with preheated and magnetized fuel before implosion.

$$C_R \approx \left(\frac{4.6\times 10^5\,\theta_{ig}^{3/2}}{V_p^3}\right)^{1/g}. \tag{3}$$

Large convergence ratios make a capsule susceptible to drive asymmetries. The tolerable variation in drive symmetry is given approximately by the expression[25] $\delta P_{\text{drive}}/P_{\text{drive}} < 1/[4(C_R-1)]$. The outer surface of a magnetically driven liner will be susceptible to the magneto-Rayleigh-Taylor (MRT) instability, which will produce irregularities on the outer surface of the liner. This will result in a drive asymmetry, since the magnetic pressure varies as r^{-2}. Equation (3)

Downloaded 18 Jan 2011 to 134.253.26.11. Redistribution subject to AIP license or copyright; see http://pop.aip.org/about/rights_and_permissions

indicates a cylindrical implosion requires $C_R \sim 120$ while a spherical implosion requires only $C_R \sim 24$ for an implosion velocity of 10 cm/μs and an ignition temperature of 10 keV, demonstrating the clear advantage of spherical over cylindrical implosions. Equation (2) indicates that starting the implosion with preheated fuel reduces the convergence ratio required to reach the ignition temperature, e.g., only a cylindrical convergence of 18 is required when the fuel is preheated to 200 eV.

Equation (3) indicates that high velocity implosions do not require either preheat or high convergence. However, such implosion velocities are difficult to obtain with pulsed-power-driven liners due to the relatively long pulse length ($\sim$100 ns) as compared to the implosion time (10–20 ns) of typical ICF capsules. We further illustrate this point using an analytic liner implosion solution.[26] The radius of the liner as a function of time is given by the expression

$$r = r_0(1 - \tau^4), \tag{4}$$

where the current drive is of the form $I = I_x(27/4)^{1/4}\tau \times (1-\tau^4)^{1/2}$, I_x is the peak current, $\tau = t/t_p$, t_p is the length of the current pulse, and the units are mks. Note the peak current occurs when $t = t_x = t_p/3^{1/4} \approx 0.76 t_p$. The initial outer radius of the liner is given by the expression

$$r_0 = \frac{1}{2}\left[\frac{3\mu_0 A_R}{2\rho_L(2 - 1/A_R)}\right]^{1/4}\left(\frac{I_x t_x}{\pi}\right)^{1/2}, \tag{5}$$

where $A_R = r_0/(r_0 - r_i)$ is the aspect ratio of the liner, thus $r_0 = 3.39$ mm for $I_x = 25$ MA, $t_x = 100$ ns, $A_R = 6$, $\rho_L = 1.85$ g/cc for beryllium. Note that we have chosen beryllium for the liner material because it is a strong low density metal. This allows the use of low aspect ratios, which should be more robust against instabilities. Furthermore, the yield degradation due to the inevitable mix of this material into the fuel is minimized because it is low Z. The implosion velocity is obtained by taking the derivative of Eq. (4) and combining with Eq. (5). The maximum liner velocity will be approximately

$$v = 6.4\left\{\frac{A_R}{[1 - 1/(2A_R)]}\right\}^{1/4}\left(\frac{I_x}{25\ \text{MA}}\frac{100\ \text{ns}}{t_x}\right)^{1/2} \text{cm}/\mu\text{s}. \tag{6}$$

This expression, which yields 10.2 cm/μs for $I_x = 25$ MA, $t_x = 100$ ns, and $A_R = 6$, depends very weakly on the liner aspect ratio and rather weakly on the current and implosion time. This indicates that much larger peak currents and/or shorter pulse lengths would be necessary to achieve implosion velocities greater than 20 cm/μs for a liner with an aspect ratio of 6. It is unlikely[27] that fast liners with aspect ratios much greater than 6 can be imploded without disruption due to the MRT instability without techniques to control instability. Note that liners can remain unmelted during slow implosions and thus retain material strength. This can allow the use of higher aspect ratios. Proper pulse shaping and adiabatic compression may allow fast liner implosions to retain strength during at least a portion of the implosion, which could reduce the overall growth of the MRT.

So far, we have only considered adiabatic compression, but other heating and cooling mechanisms are important during the implosion. The temperature of the fuel is determined by the balance of heating and loss rates as expressed by the formula

$$C_V\frac{dT}{dt} = G_{PdV} - L_{\text{rad}} - L_{\text{cond}} + G_\alpha, \tag{7}$$

where $C_V = 3NK/2$ is the heat capacity of an ideal gas with a total of N particles (electrons and ions when fully ionized), G_{PdV} is the energy gain due to compression, L_{rad} is the loss due to radiation, L_{cond} is the loss due to thermal conduction, and G_α is the gain due to α-particle deposition.

If we assume a cylindrical implosion with uniform fuel density and use the ideal gas equation of state, the rate of compressive heating is given by the expression

$$P\frac{dV}{dt} \approx 5.0 \times 10^8 \Gamma \theta \frac{dr}{dt}\ \text{W/cm}, \tag{8}$$

where $\Gamma = \rho r$ in g/cm^2, and r is the outer radius of the fuel in cm. If we ignore G_α and the losses, Eq. (7) yields

$$\theta = \theta_0(r_0/r)^{4/3}, \tag{9}$$

which is consistent with Eq. (2) as expected for the adiabatic heating of a cylinder.

The energy lost by thermal conduction (cgs) is given by the expression

$$L_c = 2\pi r k_c \nabla(kT) \approx 2\pi k_c kT, \tag{10}$$

where k_c is the conductivity coefficient and we have assumed $\nabla kT \approx kT/r$. Electrons conduct heat very effectively due to their low mass and subsequent high velocity. Thus electron thermal conductivity dominates the conductivity of ICF plasmas. This term must be significantly smaller than the heating term of Eq. (8) if the ignition temperature is to be attained during compression. Since the hydrodynamic heating rate is proportional to the implosion velocity, there is a minimum implosion velocity of about 20 cm/μs required for standard ICF capsules.[28] Inhibiting the thermal conductivity could dramatically reduce this minimum velocity.

The presence of a strong magnetic field inhibits the electron transport of thermal energy in the direction perpendicular to the magnetic field, but not along the field lines. This is because the electrons gyrate about the magnetic field lines, but are free to move along the field lines. The degree of magnetothermal-insulation is a function of the Hall parameter, which is the product $\omega_{ce}\tau_e$, where $\omega_{ce} = eB/m$ is the cyclotron frequency of the electrons and τ_e is the average time between electron-ion collisions. The conductivity including the effect of a transverse magnetic field (cgs) is given by the expression[29]

$$k_{ce} = 3.16 n\frac{kT}{m_e}\tau_e\left(\frac{1 + 0.39x_e^2}{1 + 3.9x_e^2 + 0.26x_e^4}\right), \tag{11}$$

where $x_e = \omega_{ce}\tau_e$. If we assume the electron collision time is determined by collisions with the background ions then $\tau_e = \tau_{ei} \approx 1.1 \times 10^{10}\theta^{3/2}/(n \ln \Lambda)$. The energy lost from a cylinder of DT by electron conductivity (assuming $\ln \Lambda = 7$) is

Downloaded 18 Jan 2011 to 134.253.26.11. Redistribution subject to AIP license or copyright; see http://pop.aip.org/about/rights_and_permissions

$$L_{ce} \approx 8.7 \times 10^{12} \theta^{7/2} \left(\frac{1 + 0.39 x_e^2}{1 + 3.9 x_e^2 + 0.26 x_e^4} \right) \text{ W/cm}, \quad (12)$$

where $x_e = \omega_{ce}\tau_e = .0011\theta^{3/2}B/\rho$ (B in T and ρ in g/cc). There is potentially a large reduction in the energy lost by thermal conduction when the plasma is magnetized. This enables the attainment of ignition temperatures with slow implosions. We note that the axial magnetic field does not reduce the electron conductivity in the axial direction. However, the energy lost by axial heat flow is much smaller than the energy lost in the radial direction because the fuel volume is compressed into a long thin cylinder ($r_f \sim 100$ μm, $L \sim 5000$ μm) and most of the heat is lost when the fuel is nearly fully compressed, since the conductivity is proportional to $\theta^{7/2}$. The axial heat flow must exit through a small area, $A_{\text{axial}} = 2\pi r_f^2$, whereas the radial flow exits through a much larger area, $A_{\text{radial}} = 2\pi r_{\text{fuel}} L$. Furthermore, the axial temperature gradient is proportional to $1/L$, while the radial temperature gradient is proportional to $1/r_f$. Thus the ratio of the radial to axial thermal heat loss is roughly $(L/r_f)^2 \approx 2500$. According to Eq. (11), this implies that the axial losses would be comparable to the radial losses if the effective value of $x_e = 60$, which is consistent with the results of numerical simulations presented in the next section. We are developing the capability to model the complete liner system, including end walls and laser heating. We plan to present such simulations, which will self-consistently calculate end losses, in a future publication.

When the electron conductivity has been strongly inhibited by a large magnetic field, ion conductivity must be considered. The power lost from a cylinder of DT through ion conductivity is given approximately by the expression

$$L_{ci} \approx 1.7 \times 10^{11} \theta^{7/2} \left(\frac{1 + 0.756 x_i^2}{1 + 3.99 x_i^2 + 1.48 x_i^4} \right) \text{ W/cm}, \quad (13)$$

where $x_i = \omega_{ci}\tau_i = 1.7 \times 10^{-5}\theta^{3/2}B/\rho$, where B is in T and ρ is in g/cc.

Equations (12) and (13) indicate that as B/ρ becomes large, $L_{\text{cond}} = L_{ce} + L_{ci}$ becomes small. However, the compressive heating must still be much larger than the radiation losses. The radiation loss rate for a cylindrical volume of DT fuel, which is dominated by bremsstrahlung,[30] is given by the formula

$$L_{\text{rad}} \approx 9.6 \times 10^{16} \Gamma^2 \theta^{1/2} \text{ W/cm}. \quad (14)$$

Combining Eqs. (4), (5), (8), and (14), we find that $\rho_0 \ll 2.1 \times 10^{-8} (\theta_0^{1/2}/t_x)(r/r_0)^{1/3}(1 - r/r_0)^{3/4}$ g/cc. This constraint is the most important at the end of the implosion. If we assume a required ignition temperature of 10 keV and use Eq. (9) to determine r_f/r_0, we obtain

$$\rho_0 \ll 1.2 \times 10^{-8} \frac{\theta_0^{3/4}}{t_x} \text{ g/cc}. \quad (15)$$

Thus, the initial fuel density must be much less than 20 mg/cc for an initial preheat temperature of 100 eV and an implosion time of 100 ns. The numerical solutions indicate that the optimal initial fuel density is 1–5 mg/cc for Z-machine driven implosions, which is consistent with this result. Note that lower fuel densities are required for slower implosions.

The relatively short implosion time of 100 ns for the Z machine provides two advantages compared to longer implosion times (>10 μs) previously considered for MTF such as the FRC experiments. The relatively high fuel density after compression allows the use of a purely axial magnetic field, which can only inhibit the radial transport of the α-particles. Thus the minimum axial length of the liner to obtain significant axial α-particle trapping is determined approximately by the formula

$$\rho \Delta z \geq 0.5 \text{ g/cm}^2, \quad (16)$$

where Δz is the length of the liner. Simulations indicate that pulsed power liner implosions with optimal yields have final fuel densities of 0.5–1.0 g/cc. According to Eq. (16) the liner must have a modest length of 0.5–1.0 cm. In comparison, 10 μs liner implosions would have large inductance due to a required a length of 50–100 cm, requiring high driving voltages. Thus a simple axial magnetic field is not suitable for long time scale implosions. In addition, the energy required to preheat the fuel scales unfavorably as the implosion time is increased. Combining the expression for the fuel mass $M_{\text{fuel}} = \pi r_0^2 \rho_0 \Delta z$ with Eqs. (5) and (16), we find the following expression for the required preheat energy

$$E_{\text{preheat}} \approx 3.4 \theta_0 I_x t_x \left(\frac{r_f}{r_0} \right)^2 \left[\frac{1.85 g/cc}{\rho_{\text{liner}}} \frac{A_R}{2 - 1/A_R} \right]^{1/2} \text{kJ}. \quad (17)$$

This equation implies a preheat energy of 6.5 kJ for a peak current $I_x = 25$ MA, a time to peak current, $t_x = 100$ ns, $A_R = 6$, and a preheat temperature of 100 eV. This modest energy could be provided by the Z-Beamlet laser as illustrated in Fig. 1. In contrast, the preheat energy of 650 kJ required for a 10 μs implosion would require a very expensive laser or another means to heat the fuel. Thus our proposed approach of using a simple axial magnetic field for fuel magnetization and a laser to preheat the fuel is presently practical only for relatively short implosion times, which are made possible by pulsed power machines such as the Z machine.

B. Fusion self-heating

The DT fusion reaction generates a 14.1 MeV neutron and a 3.5 MeV α-particle (He^4). In ICF capsules, nearly all of the neutron energy escapes and only the α-particles heat the fuel. The fusion rate is proportional to the velocity-averaged fusion cross section,[31] which can be approximated by the power law fit $\langle \sigma v \rangle \approx 2.74 \times 10^{-19} \theta^{2.6}$ cm^3/s to better than 5% over the temperature range 7–13 keV. The α-heating rate using this approximation is given by the equation

$$P_\alpha \approx 7.4 \times 10^{15} \Gamma^2 \theta^{2.6} f_\alpha \text{ W/cm}, \quad (18)$$

where f_α is the fraction of α-particle energy deposited into the fuel. The range of α-particles in DT is given approximately[32] by the expression $\Gamma_\alpha \approx 0.015\theta^{3/2}$ g/cm^2 (0.2–0.4 g/cm^2 for $\theta = 5$–10 keV). Consequently, the product of the fuel density times the fuel radius, called the areal density ρr, must be of this order for ignition, i.e.,

Downloaded 18 Jan 2011 to 134.253.26.11. Redistribution subject to AIP license or copyright; see http://pop.aip.org/about/rights_and_permissions

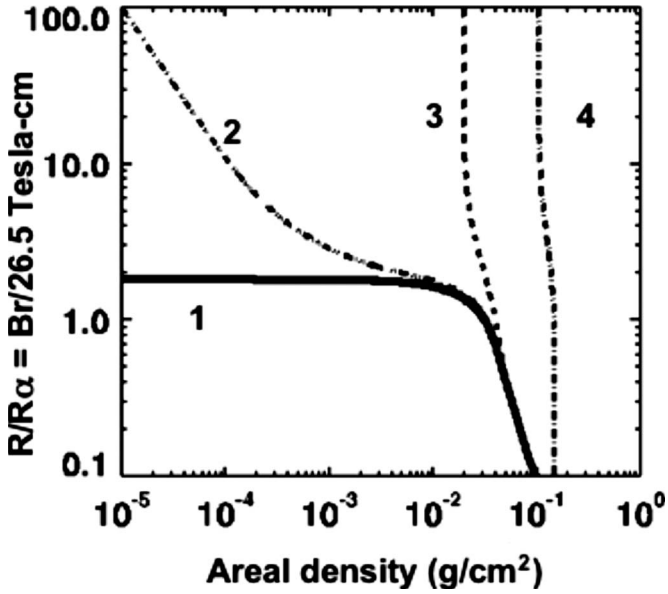

FIG. 2. Magnetized fuel ignition space contours are plotted as a function of fuel areal density and the ratio of the cylinder radius over the cyclotron radius of a fusion α-particle with its initial energy as calculated with the following assumptions, (1) α transport including B-field effects and classical magnetic conductivity inhibition, (2) α-transport including B-field effects and Bohm magnetic conductivity inhibition, (3) α transport ignoring B-field effects and classical magnetic conductivity inhibition, and (4) α transport including B-field effects and conductivity ignoring B-field.

$\rho r \approx 0.3$ g/cm^2, unless the fuel is magnetized. It is difficult to satisfy this condition and Eq. (15) simultaneously, e.g., a convergence ratio of over 300 is required for a liner with an initial radius of 3 mm and fuel density of 3 mg/cc. The challenge of needing high fuel areal density can be overcome by fuel magnetization. The addition of a magnetic field in the fuel causes the α-particles to follow helical paths. This increases the fraction of the α-particle energy deposited in the fuel before escaping as indicated by the formula[32]

$$f_\alpha \approx \frac{x_\alpha + x_\alpha^2}{1 + 13x_\alpha/9 + x_\alpha^2}, \quad \text{where}$$
$$x_\alpha = \frac{8}{3}\left(\frac{\rho r}{\Gamma_\alpha} + \frac{b^2}{\sqrt{9b^2 + 1000}}\right), \tag{19}$$

where $b = r/r_\alpha$, $r_\alpha = 26.5/B$ cm/T is the gyro radius of an α-particle with 3.5 MeV, and r is the radius of the cylindrical fuel volume in cm.

Thermonuclear ignition can occur only when the α-heating is larger than the sum of the losses due to radiation and thermal conduction. This ignition space is often plotted as a function of the fuel areal density and temperature. We present in Fig. 2 a plot of the ignition space with a fixed fuel temperature of 10 keV as a function of ρr and $r/r_\alpha = Br/26.5$ T cm. The solid curve labeled 1 is determined by balancing α-heating against the losses [Eqs. (12), (14), (18), and (19)]. This curve illustrates the tradeoff between fuel ρr and the product Br when transitioning from traditional ICF with no magnetic field to inertial fusion with magnetized fuels. This curve intercepts the $\rho r = 0$ axis indicating that given $r/r_\alpha > 1.8$ ($Br > 47.7$ T cm) ignition is possible for any fuel ρr at 10 keV temperature. Note that in the limit of large $\omega_{ce}\tau_e$, the conductivity loss given by Eq. (12) scales as $1/B^2$ as does the classical diffusion equation for particles contained by a magnetic field. Experiments with magnetically confined plasmas have shown that particles can diffuse faster than would be expected by classical diffusion. This anomalous diffusion is believed to be due to fluctuations generated by plasma instabilities. Due to strong collisionality,[33] it is unlikely that the cross-field transport will exceed the Bohm value obtained by the substitution $\tau_e = 16/\omega_{ce}$ into the classical diffusion coefficient when $\tau_{ei} > 16/\omega_{ce}$. To determine the importance of this type of anomalous transport of the electron thermal conduction on the ignition space, we make this same substitution into Eqs. (11) and (12), with the resulting curve labeled 2. Note that this curve does not intercept the $\rho r = 0$ axis at finite Br. However, we expect $\rho r > 0.001$ g/cm^2 for liners driven by the Z machine, where there is little deviation of curve 2 from curve 1 and thus such liner implosions should be robust to Bohm-like anomalous diffusion. We obtained the curve 3 by including the effect of the B-field on the classical thermal conductivity, but not including its effect on the α-deposition. We obtained curve 4 by including the effect of the magnetic field on the α-particle deposition, but not on the electron thermal conductivity. Curve 4 indicates that the required fuel ρr is not strongly decreased simply by increasing the α-deposition. Clearly inhibiting thermal conductivity has a much stronger effect on the required ρr, but it is the combination of both these effects that produces the significant alteration in the ignition space that is indicated by either curves 1 or 2.

C. Inertial confinement and gain

To obtain gain greater than unity, the fusion fuel must be confined long enough to allow sufficient fusion reactions to occur. In conventional ICF the areal density of the fuel provides this confinement. In contrast, the areal density of the liner must provide most of the confinement for magnetized fuels since the fuel areal density can be very small. The motion of the liner near stagnation can be calculated using Newton's equation. We ignore the magnetic force driving the liner inward and assume that the accelerating force arises only from the fuel pressure, which can easily be determined if adiabaticity is assumed. Further assuming that the liner is thin we obtain $\ddot{x} = 1/(x^{7/3}\tau_s)$, where $\tau_s = (0.1\Gamma_L/P_s)^{1/2}$, $x = r/r_s$, and r_s, P_s, Γ_L are the fuel radius, fuel pressure, and liner areal density at stagnation. The first integral of this equation yields the velocity, $\dot{x} = (1/\tau_s)[1.5(1 - x^{-4/3})]^{1/2}$. The fusion yield can then be obtained from the integral $Y_{\text{fusion}} = \int \dot{E}_{\text{fusion}} dt$, where $\dot{E}_{\text{fusion}} = 5P_\alpha/f_\alpha$, P_α is given by Eq. (18), and $dt = dx/\dot{x}$. We obtain $Y_{\text{fusion}} = 3.2 \times 10^{11}(\rho_s r_s)^{3/2} r_s \Gamma_L^{1/2} \theta_s^{2.1}$ J/m. The energy of each particle in a fully ionized plasma is approximately 3/2 kT, which implies the energy in the fuel at stagnation is given by $E_{\text{fuel}} = 3.8 \times 10^{10} \rho_s r_s^2 \theta_s$, where ρ_s is the fuel density at stagnation. Defining the gain, $Q \equiv Y_{\text{fusion}}/E_{\text{fuel}}$, we obtain the result

Downloaded 18 Jan 2011 to 134.253.26.11. Redistribution subject to AIP license or copyright; see http://pop.aip.org/about/rights_and_permissions

$$Q = 8.4(\Gamma\Gamma_L)^{1/2}\theta_s^{1.1}. \tag{20}$$

It is interesting that the gain increases with both the areal density of the fuel and the liner, despite the fact that the magnetized fuel ignition space includes very small fuel areal densities (see Fig. 2). This is because burn rate depends on the fuel areal density. The gain can be determined as a function of liner and implosion parameters. An expression for the fuel density is obtained from Eq. (15) by normalizing to the optimum initial fuel density of about 3 mg/cc found numerically. Then using Eqs. (2), (5), (6), and (9), we obtain

$$Q = 4.5 \times 10^{-11}\left(\frac{\rho_L}{A_R}\right)^{0.7}\left(\frac{C_R}{t_x}\right)^{0.4} I_x. \tag{21}$$

This formula indicates $Q=1$ is obtained for a drive current of 22 MA for a beryllium liner with $A_R=6$, $t_x=100$ ns, and $C_R=25$. The numerical simulations of the next section indicate that a somewhat higher drive current of about 36 MA is needed due to nonideal effects. However, the gain will increase faster than indicated by Eq. (21) when α-self-heating becomes important.

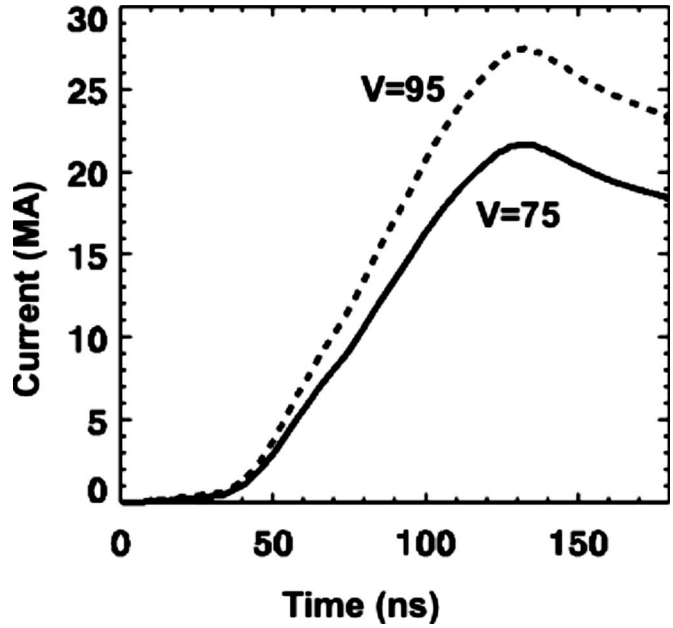

FIG. 3. Current profiles generated by the Z machine, for two Marx bank charging voltages (kilovolts), are plotted as a function of time.

III. NUMERICAL SIMULATIONS AND YIELD SCALING

We performed a study of the potential performance of magnetized liners using the simulation code Lasnex.[34] This code is well-benchmarked to inertial fusion experiments. It can simulate radiative transport coupled with magnetohydrodynamics, contains a circuit model allowing the drive current from the Z machine to be self-consistently calculated with the simulated load (magnetized liner), and includes the effect of magnetic fields on thermal conductivity and the transport of the α-particles. Note that test problems were run, which were in agreement with Eq. (19). Detailed models of the equation of state and the electrical resistivity were used for the liner material, which was chosen to be beryllium in this study for the reasons previously mentioned. These capabilities allowed us to start the simulations at room temperature. Thus the effect of joule heating, melting, and vaporization of the liner material were calculated. Present fabrication techniques result in an rms surface roughness of approximately 60 nm, which was initialized at the surfaces of the liner in our two-dimensional (2D) simulations. The geometry of the magnetized liner is shown in Fig. 1. The current from the Z machine flows on the outside of the tubular liner and generates an azimuthal field that exerts a pressure on the liner given by the expression $P_{\mathrm{Mag}}=B^2/2\mu_0=\mu_0 I^2/8\pi^2 r^2$. An equivalent circuit model of Z was used to drive the liner in all our simulations. The expected drive currents are shown in Fig. 3 for two different Marx bank charging voltages. Indications are that Z should provide a peak current of approximately 27 MA when the machine is fired at a charging voltage of 95 kV. Note that this implies a magnetic pressure of approximately 100 Mbar when the liner outer radius is 1 mm, i.e., before the liner is fully imploded. This corresponds to the ablation pressure of a radiation driven ICF capsule at 272 eV. The simulations were started with an initial axial magnetic field and the evolution of this field was followed self-consistently. Energy was deposited into the fuel over a 10 ns period (to mimic the laser deposition) beginning approximately 50 ns after the drive current started. The total energy deposited was chosen to give the desired preheat temperature for a particular simulation. The energy was deposited uniformly throughout the fuel in this initial study. In the next section, we show that there are advantages (including higher yield) to heating only a central portion of the fuel. A large number of one-dimensional (1D) simulations were performed to determine the scaling of these magnetized liners. We are working toward a point design for the Z machine. The preliminary point design parameters are as follows. The beryllium liner has an initial outer radius of 3.48 mm, an axial length of 5.0 mm, and an aspect ratio $A_R \equiv r_o/(r_o-r_i)=6$. A peak drive current of 27 MA results in a convergence ratio of 25 for DT fuel with an initial density of 3 mg/cc, which is preheated to 250 eV and embedded with an initial magnetic field of 30 T. This implosion results in a final on-axis fuel density of 0.5 g/cc, peak fuel temperature of 8 keV, peak fuel pressure of 3 Gbar, final field of 130 MG, and a 1D yield of 500 kJ. Other parameters of interest are the peak value of the ratio $r/r_\alpha > 3$, the peak fuel $\rho r \sim 0.01$ g/cm^2, the peak Hall parameter $\omega_{ce}\tau_e > 200$, and the peak liner $\rho r = 1.3$ g/cm^2. We note the ρr of the liner is comparable to the high-density ρr of the NIF capsule design. It is the ρr of the liner that provides the inertial confinement in our scheme, not the fuel ρr as in the NIF capsule design.

The average fuel radius, drive current, and average fuel ion temperature (near $r=0$) are plotted as a function of time in Fig. 4. Notice that the ion temperature rises to approximately 200 eV due to the preheating, which is timed to occur when the liner just starts to implode ($t \sim 80$ ns). The ion temperature peaks when the fuel radius reaches the minimum value. The ion temperature, magnetic field strength, and fuel density at stagnation (maximum compression and peak burn rate) for two simulations are plotted as a function of the fuel

Downloaded 18 Jan 2011 to 134.253.26.11. Redistribution subject to AIP license or copyright; see http://pop.aip.org/about/rights_and_permissions

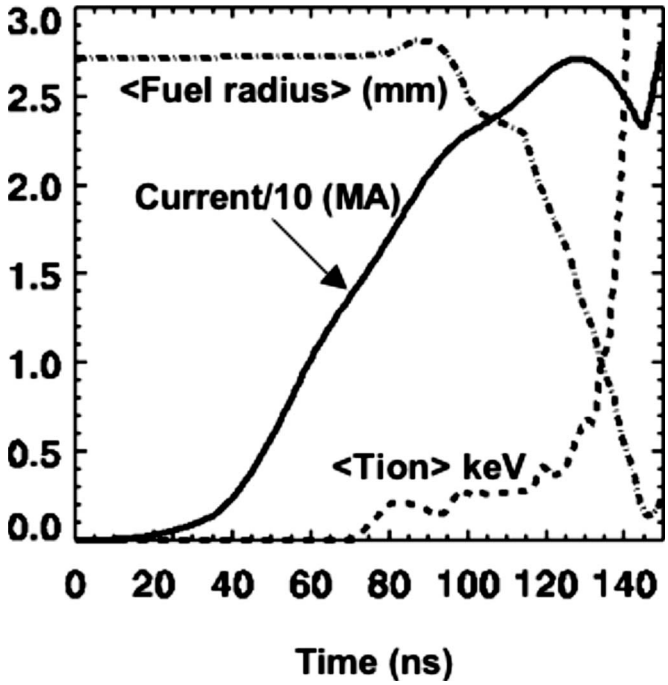

FIG. 4. Several normalized parameters are plotted as a function of time. The results are from a Lasnex simulation of a beryllium liner with an aspect ratio of 6, an initial magnetic field of 30 T, an initial fuel density of 3 mg/cc, and an initial fuel temperature of 250 eV. The yield was about 500 kJ for a 0.5 cm long liner.

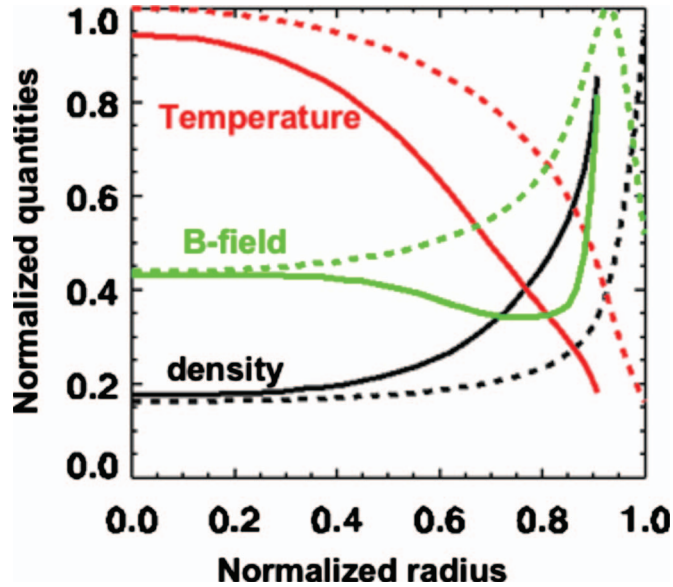

FIG. 5. (Color) Normalized parameters simulated by Lasnex are plotted as a function of normalized radius. The solid lines are with the Nernst term included. The simulation parameters were the same as Fig. 4.

radius in Fig. 5. The solid curves are for a simulation including the Nernst term, which affects the magnetic field when a perpendicular temperature gradient exists. The Nernst effect causes the magnetic field to be transported out of the plasma even when it is a very good conductor (as is true in these simulations where magnetic Reynolds numbers from 2000–20 000 exist within the fuel). When the plasma is highly magnetized the time derivative of the magnetic field strength due to the Nernst term is given by the formula $dB/dt = \{\nabla \times [B \times \nabla(kT)]\}/e|B|\omega_{ce}\tau_e$. The dashed curves are for a second simulation, where the Nernst term has been ignored. All radii are normalized to the outer fuel radius of the second simulation. Similarly the densities, temperatures, and magnetic fields are normalized to the corresponding peak values in the second simulation (without Nernst). The initial magnetic field in these simulations was 10 T. Approximately 70% of the magnetic flux initially introduced into the fuel is lost when the Nernst term is included, as compared to about 25% when the Nernst term is ignored. Furthermore the inclusion of the Nernst term decreases the fusion yield by about 70%. Note the simulation with the Nernst term is more compressed due to the subsequent reduction in the magnetic pressure within the fuel. Clearly the inclusion of the Nernst term has a significant effect on these profiles and needs to be included in simulations of magnetized fuel. However, the strength of the Nernst effect is inversely proportional to the Hall parameter and becomes less important as the applied magnetic field is increased. For example, the flux lost with the Nernst effect drops from 70% to about 45% when the initial field is raised from 10 to 30 T.

To study the scaling of this concept for currents in excess of Z's capabilities the model drive voltage was scaled accordingly. The results from simulations with a peak current of 30 MA are shown in Fig. 6. The 1D-simulated fusion yield per centimeter is plotted as a function of the fuel preheat temperature in Fig. 6(a) for a beryllium liner with an initial aspect ratio of 6 and initially magnetized with a 30 T magnetic field. At each initial preheat temperature the initial fuel density is chosen so that the liner will implode to a desired convergence ratio. These densities are plotted in Fig. 6(b). Note that the yield is very small for preheat temperatures less than 100 eV and there is an optimal preheat temperature for each of the convergence ratios. The peak yields are larger for the larger convergence ratios; however, the risk of liner disruption due to instabilities is correspondingly higher. In consideration of this, we have chosen a modest convergence ratio of about 25 for our point design.

The 1D-simulated fusion yield per centimeter is plotted as a function of initial applied magnetic field strength in Fig. 7. The drive current and liner aspect ratio are the same as in Fig. 6. The initial fuel preheat temperature was chosen to maximize the yield, while the initial fuel density was chosen to obtain the labeled convergence ratios. Note that the yield is very small at small magnetic fields (although the fuel has been preheated) and for each of these curves the yield increases almost exponentially with field strength. The curves with convergence ratio 20 and 30 have a global maximum value, i.e., an optimum initial magnetic field. Peak yield occurs when the pressure of the applied magnetic field becomes approximately equal to the material pressure when the liner has stagnated. Continuing to increase the applied magnetic field above this value simply results in putting a larger fraction of the liner implosion energy into compressing the field and not into compressing the fuel, which must then be at a reduced density to maintain the same convergence ratio thus leading to a decreased yield. We expect that the curve for aspect ratio 10 has a maximum yield at an initial magnetic

Downloaded 18 Jan 2011 to 134.253.26.11. Redistribution subject to AIP license or copyright; see http://pop.aip.org/about/rights_and_permissions

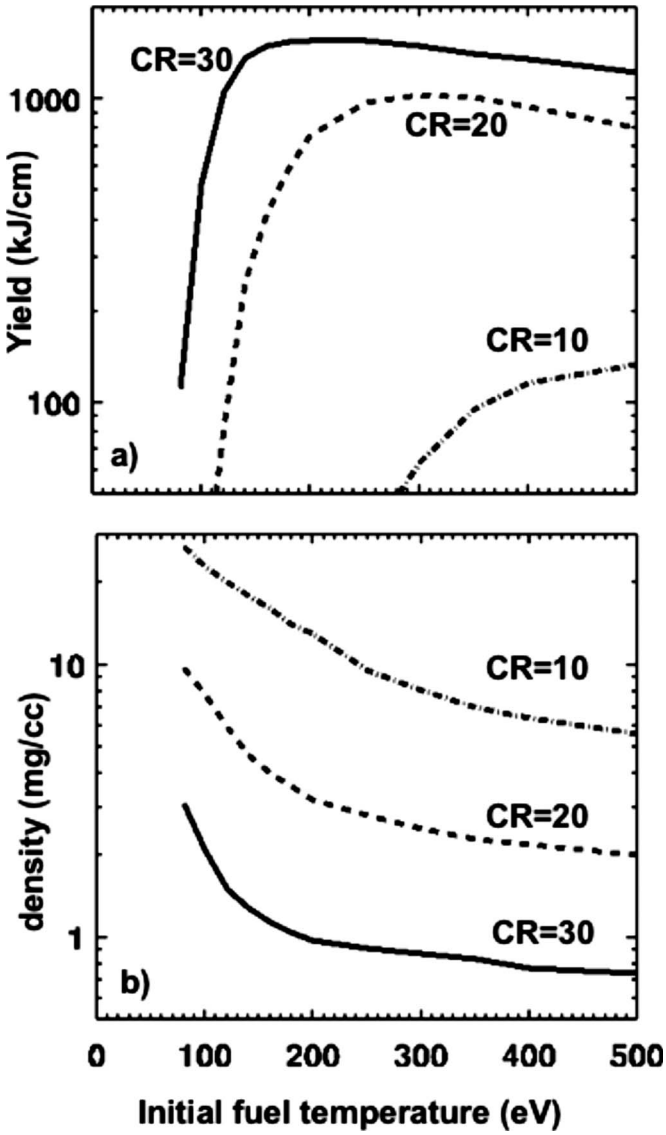

FIG. 6. The yields from 1D Lasnex simulations of beryllium liners with aspect ratio 6 with a peak current drive of 30 MA are plotted as a function of the initial preheat temperature in (a). The corresponding initial fuel densities to obtain the convergence ratios of each curve are plotted in (b).

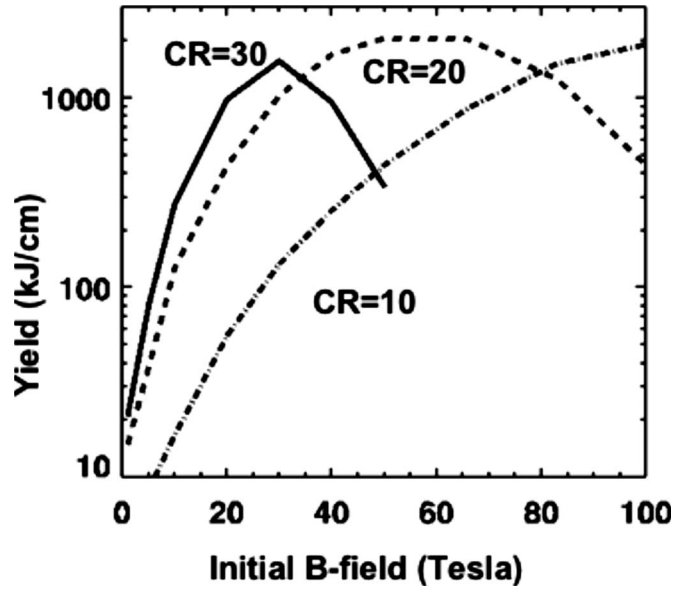

FIG. 7. 1D yield as a function of initial magnetic field for a beryllium liner with an aspect ratio=6 and a peak current drive of 30 MA is plotted as a function of initial magnetic field strength.

field in excess of 100 T (1 MG), but we did not extend the curve beyond this value because it seems unlikely that such a field could be provided in the near future. We have chosen 30 T for our point design because this is near optimum for liner implosions with convergence ratios greater than 20, and because creating such a field strength is feasible with existing coil technology. However, notice that the yields for lower convergence ratio implosions can be made just as large as the higher convergence ratio implosions as long as larger initial magnetic fields can be provided. Thus there is a design space that could allow a tradeoff between physics risk (convergence ratio) and engineering risk (providing large initial magnetic fields).

The 1D yield as a function of peak drive current is plotted in Fig. 8(a) for beryllium liners with an aspect ratio of 6 and an initial magnetic field of 30 T. The solid curve is for simulations including α-particle transport and deposition. The dashed line is the yield when the energy of the α-particles is artificially discarded. The comparison indicates the importance of α-particle heating. The ratio of the maximum fuel temperature with α-heating over the maximum temperature without α-heating is plotted as a function of current in Fig. 8(b) along with the ratio of the fusion yield over the energy absorbed in the liner. These results are for liners with aspect ratio=6, convergence ratios of 20, an initial magnetic field of 30 T, fuel preheat temperature of 250 eV, and initial fuel densities chosen to maintain the specified convergence ratio. The initial fuel densities fall in the range of 2–5 mg/cc. The yield is equal to the total energy absorbed by the liner at a peak drive current of about 35 MA. The fuel temperature is doubled by the α-particle heating (a potential definition of ignition for this concept) at a drive current of about 45 MA and corresponding yield of about 10 MJ. These 1D results are very promising and thus it is interesting to pursue this concept with more difficult 2D simulations that can capture the effects of instabilities such as the MRT instability.

A 2D Lasnex simulation was performed of a beryllium liner with an initial aspect ratio of 6 and an imposed surface roughness of 60 nm rms, which is consistent with the surface finish that can presently be obtained with diamond-machined beryllium. The resultant density contour plots are shown in Fig. 9. An enlargement of the contour plot near the stagnation is shown in Fig. 9(a). The implosion sequence is shown in Figs. 9(b)–9(d). Clearly the MRT instability has had a significant effect on the liner implosion and as a consequence the yield was approximately 86% of the 1D yield. A sequence of simulations such as this one was performed with different aspect ratios. The resulting yields are plotted as a function of aspect ratio in Fig. 10. The yields from 1D simulations, which monotonically increase with aspect ratio, are also plotted for comparison. The trend is not a surprising result since, in the absence of instability; more of the implo-

Downloaded 18 Jan 2011 to 134.253.26.11. Redistribution subject to AIP license or copyright; see http://pop.aip.org/about/rights_and_permissions

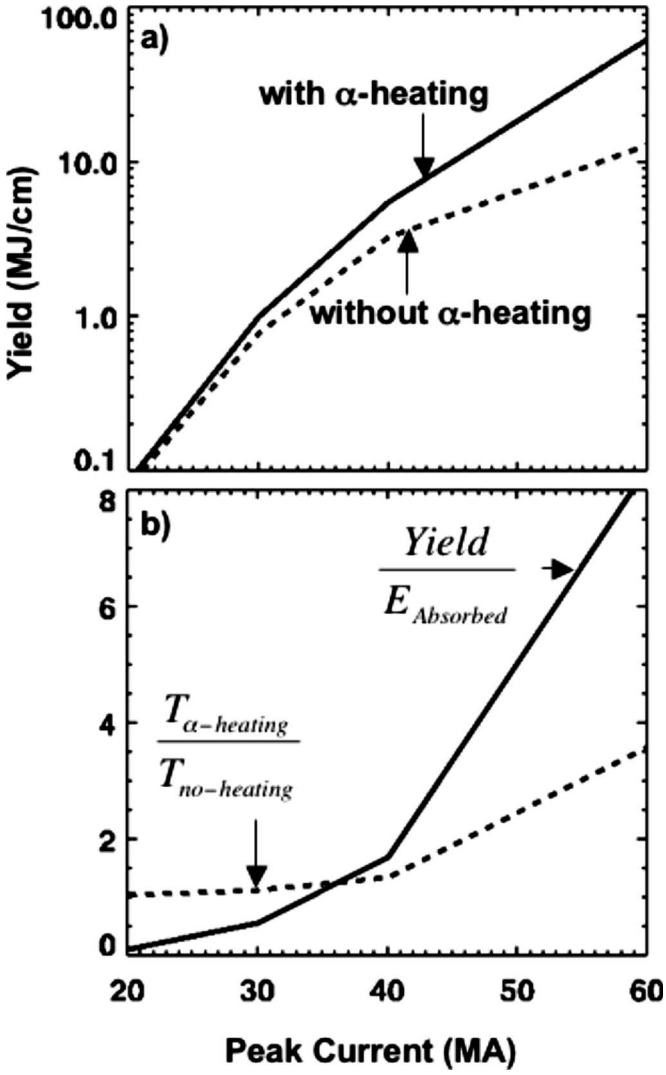

FIG. 8. (a) 1D yields are plotted as a function of maximum drive current both with (solid) and without α heating (dashed). (b) The ratio of the fusion yield over the energy absorbed in the liner (solid) and the ratio of the maximum fuel temperature with α-heating over the maximum temperature without α-heating (dashed) are plotted as a function of current. These results are for liners with aspect ratio 6, convergence ratio 20, an initial magnetic field of 30 T, fuel preheat temperature of 250 eV, and initial fuel density 2–5 mg/cc.

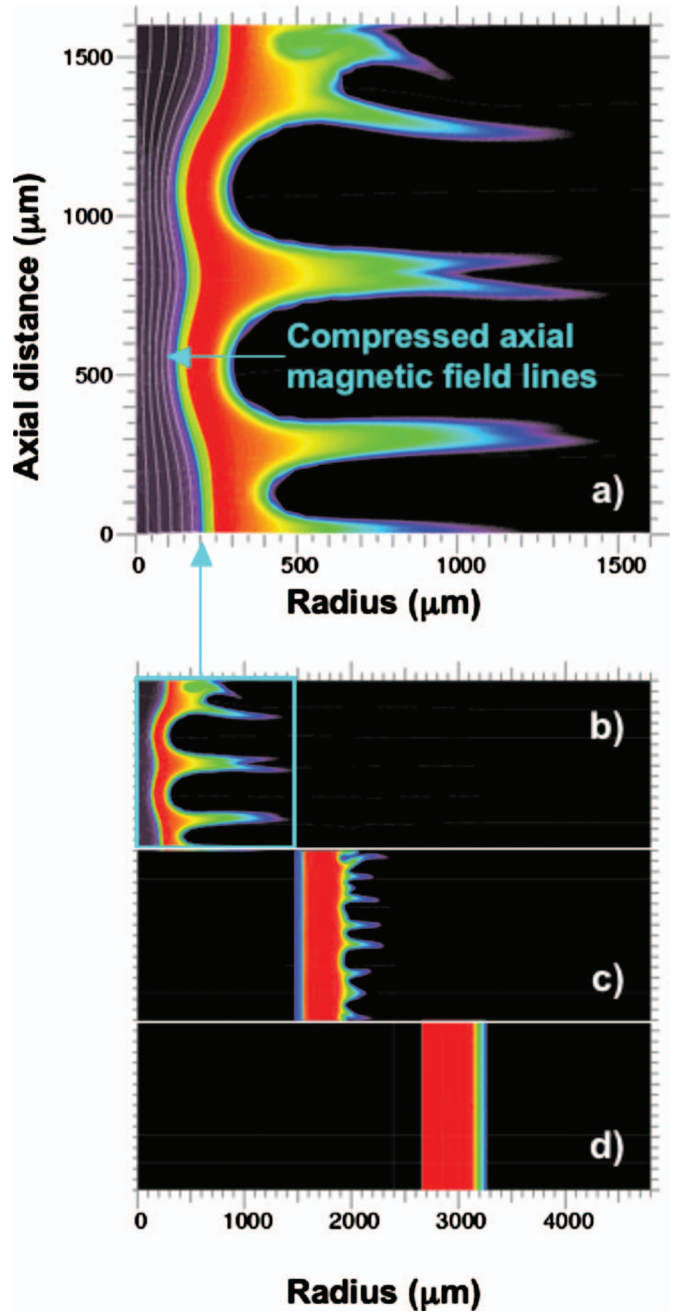

FIG. 9. (Color) 2D Lasnex simulations of a beryllium liner at (a) near stagnation (enlarged), (b) near stagnation, (c) midway, and (d) at the start of the current pulse. The liner has an initial aspect ratio 6 with a 60 nm surface roughness. The yield was approximately 86% of 1D-simulated yield.

sion energy is transferred into the fuel when the liner is made thinner. However, the 2D results indicate that there is an optimum aspect ratio near 6. This behavior is because thin walled liners are more disrupted by the MRT instability. This reduces the areal density of the liner and thus the confinement time. Thus, according to Eq. (20), we expect a reduction in the yield. We do not believe our present simulations are accurate enough to predict the optimum aspect ratio, but we do expect this basic behavior to be correct. We have varied the grid resolution and determined that submicron radial zones were required at the liner surfaces to obtain convergence in the 1D simulations. The 2D simulations presented here could resolve an axial wavelength of about 60 μm, which is much smaller than the dominant wavelengths exhibited near stagnation of about 400 μm. However, we are not sure if this axial resolution is high enough since actual liners will have roughness on scale lengths considerably smaller than 60 μm and these waves could have an effect on the evolution of the larger wavelengths through mode coupling. Note that these simulations required a significant amount of computer time (several days per simulation). Furthermore, one is never certain if the simulations have captured all the important physics. Therefore, we have started an experimental campaign to benchmark our simulations of the MRT growth. The initial results have been favorable, but much work remains. These efforts will be reported in a future publication. It should be noted that various concepts to mitigate the MRT instability can be designed and

Downloaded 18 Jan 2011 to 134.253.26.11. Redistribution subject to AIP license or copyright; see http://pop.aip.org/about/rights_and_permissions

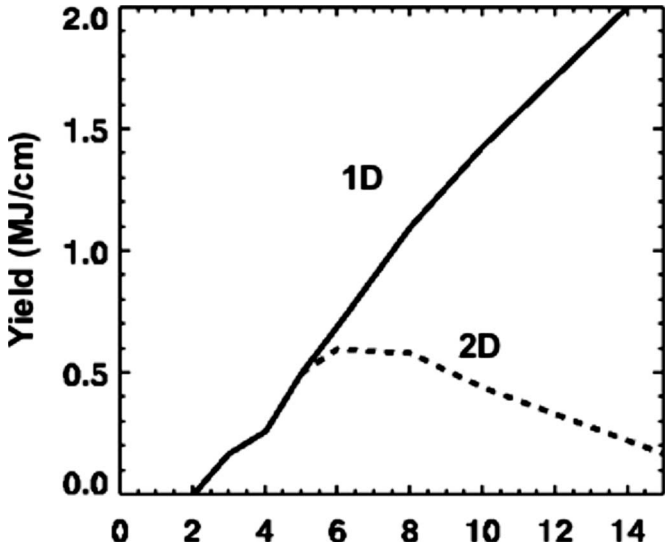

FIG. 10. The simulated 1D and 2D yields are plotted as a function of initial liner aspect ratio. These results are for liners with convergence ratios of 20, an initial magnetic field of 30 T, fuel preheat temperature of about 250 eV, and an initial fuel density 3 mg/cc.

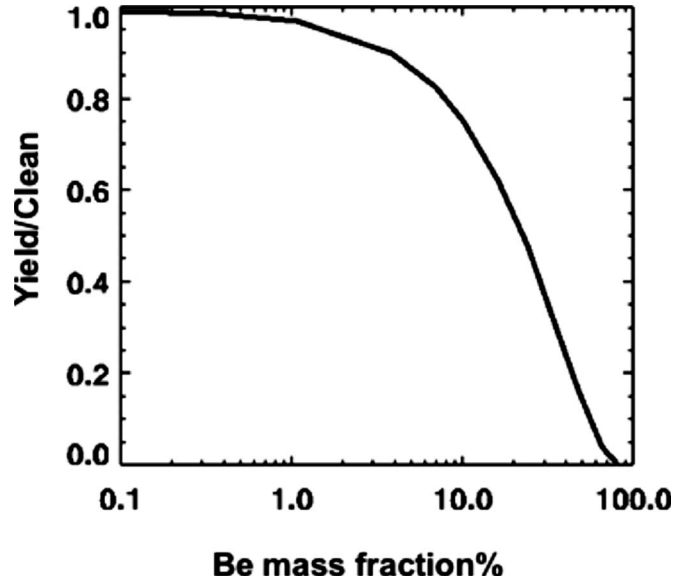

FIG. 11. Yields are plotted as a function of the mass fraction of beryllium initially mixed into the fuel. The yield is normalized to the yield with pure DT.

tested with benchmarked simulation capability and backlighting capability. These scenarios include grading the density of the liner, using multiple liners, and profiling the drive current for isentropic compression of the liner material so that material remains in the solid phase for a significant portion of the implosion.

The yield could be degraded by instability of the inner surface of the liner, which would cause some of the liner material to mix with the fuel. Since this process is very difficult to accurately simulate, we will defer such simulations to future work. However, we would like to know how sensitive the yield of magnetized fuel is to such mix. This can be accomplished by starting the simulations with some of the liner material (beryllium) premixed into the fuel. Figure 11 displays the results of such a series of simulations. The yield normalized to the yield without mix is plotted as a function of the mass fraction of beryllium premixed into the fuel. It is encouraging that the yield is relatively insensitive to mix, e.g., >50% of the clean yield is obtained with a beryllium mass fraction of 20%.

IV. FUEL PREHEAT

In the previous section we have shown that both magnetization and preheating of the fuel are critical to obtaining significant fusion yields from cylindrical liner implosions with modest convergence ratios driven by present-day accelerators such as the Z machine. In this section, we consider how one might preheat the fuel. We first make an estimate of how much energy will be needed. This preheat energy is given approximately by the simple relation $E_{PH}=C_V T_0 m_{\text{fuel}} \approx 1.2\times 10^5 T_{ev}\rho_f \pi r_f^2 \Delta z$, where C_V is the heat capacity of the DT fuel. Using values for our point design we find $E_{PH}\sim 8$ kJ.

There are a number of possible ways that the fuel could be heated. A laser or radiation from a z pinch could quickly heat a foil, which would explode and drive a shock wave into the fuel. One could also use the magnetic pressure from a pulsed power machine to drive an annular foil, which would drive a shock through the fuel. Another interesting possibility is to drive current through an array of DT ice fibers. The precursor plasma from this array could be directed into the cylinder and the stagnation shock would then heat this plasma. However, we believe the most promising approach is to heat the fuel directly with a laser. Fortuitously, the Z-Beamlet laser has about the right amount of energy.

Z-Beamlet is a neodymium glass laser typically operated at 2ω ($\lambda\sim 0.5$ μm), which corresponds to a critical density of 17 mg/cc in DT. The optimum initial fuel densities are in the range of 1–4 mg/cc, which is significantly below the critical density and thus inverse bremsstrahlung will dominate the laser absorption. The intensity of the laser light propagating through the DT gas can be found by solving the 1D transport equation[23]

$$\frac{dI}{dz}=-kI, \tag{22}$$

where $k=(\nu_{ei}\omega_p^2/c\omega_L^2)[1-(\omega_p^2/\omega_L^2)]^{-1/2}=k_0/\theta^{3/2}$, $k_0\approx 1.37\times 10^5(\rho\lambda_L Z_b)^2(1-227\rho Z_b\lambda_L^2)^{-1/2}$, I is the laser intensity, ω_p is the fuel plasma frequency, ω_L is the laser frequency, ν_{ei} is the electron-ion collision frequency, Z_b is the average ionization of the fuel, and ρ is the fuel density. Ignoring thermal conductivity and hydrodynamic motion, the heating of the fuel due to the laser light absorption is given by

$$C_V\frac{d\theta}{dt}=\frac{dI}{dz}=-kI. \tag{23}$$

Eqs. (22) and (23) have the solution $I=I_0[1-(z/z_f)]^{2/3}$, $\theta=\theta_0[1-(z/z_f)]^{2/3}$, and $\theta_0=(5k_0I_0t/2C_V)^{2/5}$, where I_0 is the laser intensity entering the fuel, θ_0 is the temperature of fuel at the entrance, z_f is the distance the laser front has penetrated into the fuel at a given time, t. Fuel temperature con-

Downloaded 18 Jan 2011 to 134.253.26.11. Redistribution subject to AIP license or copyright; see http://pop.aip.org/about/rights_and_permissions

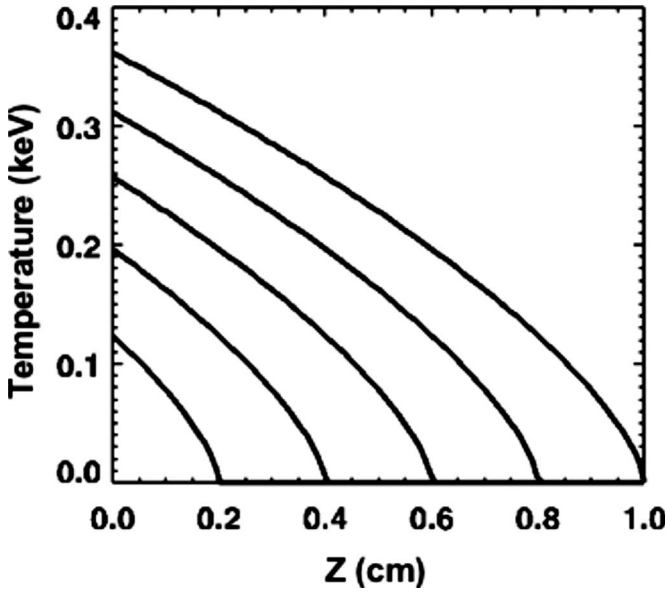

FIG. 12. Plasma temperatures as calculated from an analytic solution for laser heating, at several times, are plotted as a function of axial distance.

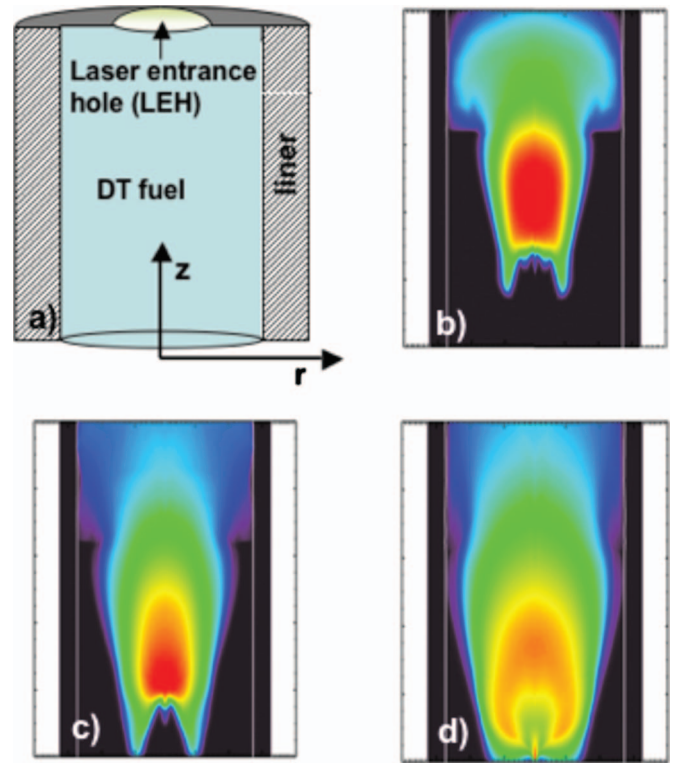

FIG. 13. (Color) (a) Schematic of the geometry for Lasnex simulations of laser heating of the fuel. Contour plots of the plasma temperature (b) $t=5$ ns, (c) $t=8$ ns, and (d) $t=11$ ns

tours given by this solution are plotted as function of distance in Fig. 12. The laser propagation can be thought of as a "bleaching wave," since the bremsstrahlung opacity drops (or is bleached) and allows the laser light to penetrate into the plasma as the gas is ionized and heated. Thus the fuel is heated to a higher temperature at the entrance than it is heated farther from the entrance, resulting in an undesirable axial temperature gradient in the preheated fuel. This analytic solution does not include thermal conductivity and hydrodynamic motion. Both of these could reduce the axial temperature gradient. We have performed 2D simulations to more fully study the fuel heating process by laser absorption. Figure 13 shows a schematic of the simulation geometry and contour plots of the simulated fuel temperature at $t=5$ ns, $t=8$ ns, and $t=11$ ns for a laser pulse length of 10 ns with a total energy of 8 kJ and a beam radius of 1 mm. Figure 14 shows the fuel temperature on axis at $t=5$ ns and $t=11$ ns. The propagation of the heating wave is clearly evident in these figures. Figure 14 also indicates that the electron and ion temperatures can be out of equilibrium during the heating phase, but will equilibrate long before the liner implodes. Apparently the combination of hydrodynamics and thermal conductivity result in a temperature profile that is more uniform than would be inferred from the simple analytical solution, compare Figs. 12 and 14. We note that numerical solutions without hydrodynamic motion and thermal conductivity agree with the analytical solution. Further work is necessary to assess the effect of axial fuel temperature gradients on performance.

Laser preheating of the fuel offers the possibility of only heating a portion of the fuel, i.e., the laser beam radius can be made smaller than the initial fuel radius. This has four immediately apparent advantages. First, the pressure that can be held by a foil covering the laser entrance hole is proportional to the foil thickness over the entrance hole radius. A small radius 1 μm thick foil can hold room temperature DT gas at 3 mg/cc. Cryogenic cooling would be required for larger radii foils. Second, the analytic solution indicates that the axial temperature gradient is smaller for fuel preheated to higher temperature. Third, for a given laser energy, the penetration depth can be matched to the liner axial extent by appropriately choosing the beam radius. Fourth, less fuel can escape out of the laser entrance hole. A sequence of 1D Lasnex simulations was performed to study the effect of varying the laser beam spot size on target performance. Surprisingly, decreasing the laser spot size increased the fusion yield and

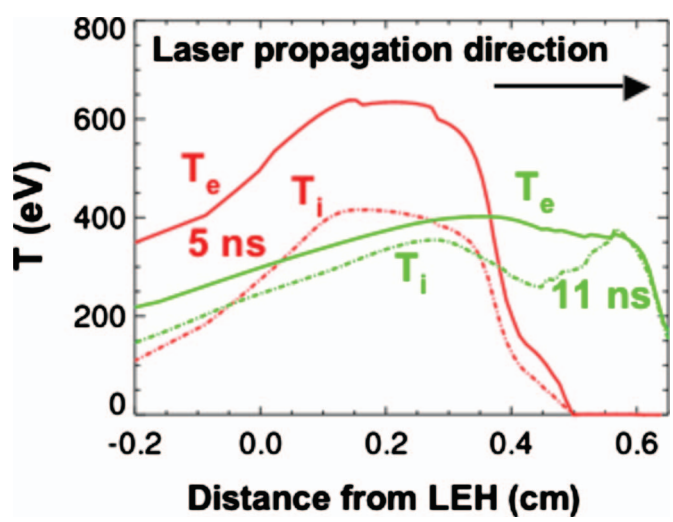

FIG. 14. (Color) Lasnex simulated laser-heated plasma temperatures at two times are plotted as a function of axial distance.

Downloaded 18 Jan 2011 to 134.253.26.11. Redistribution subject to AIP license or copyright; see http://pop.aip.org/about/rights_and_permissions

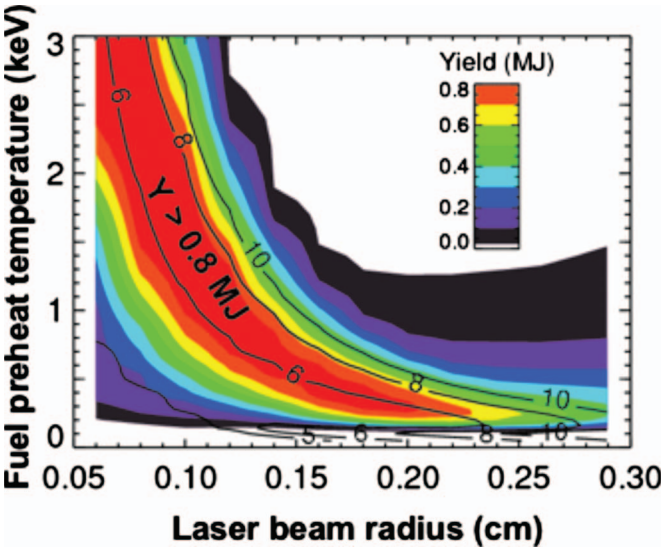

FIG. 15. (Color) Contours of the fusion yield for magnetized liners (colors) are plotted as a function of the laser beam radius and the fuel preheat temperature. The black lines are curves of the required preheat energy in kilojoules. The results are for a beryllium liner with $A_R=6$ and length $=0.5$ cm. The initial magnetic field was 30 T and the convergence ratios are fixed at 25 by adjusting the fuel density.

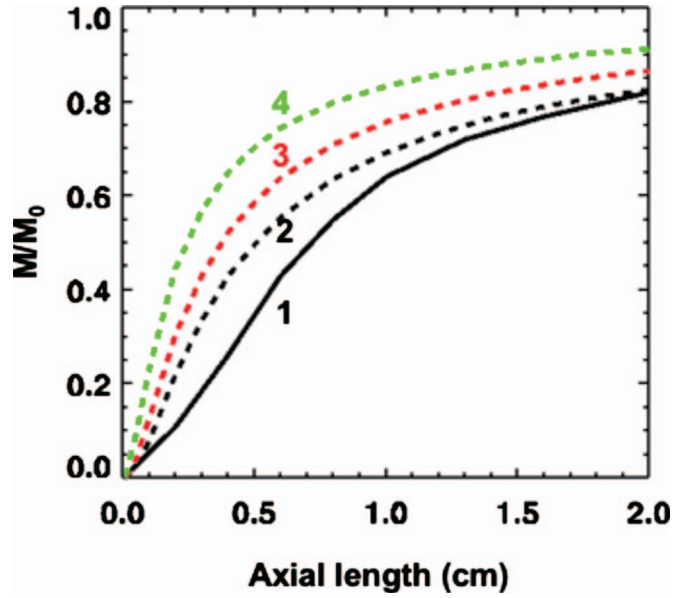

FIG. 16. (Color) The fraction of the initial fuel mass remaining at stagnation as a function of the liner length: (1) 2D numerical simulation with open end, (2) analytic result for open end, (3) analytic result for $r_H/r_0=0.5$, and (4) analytic result for $r_H/r_0=0.25$.

decreased the laser energy required. The results are summarized in Fig. 15, which shows a contour plot of the fusion yields (colors) as a function of beam radius and plasma preheat temperature within the laser beam. The black curves are contours of the required preheat energy. There is a ridge of highest yield, where the yield is about 60% larger and the fuel preheat energy is about 40% smaller than the result obtained by heating all of the fuel as was done in our scaling studies presented in Sec. II. There is little change in the yield along this ridge, but the preheat temperature varies from about 300 eV to 3 keV providing a large design space that we may explore.

Laser heating of the fuel requires one end of the liner to be essentially open. A thin foil will cover the laser entrance hole, but this foil will not be massive enough to prevent the escape of some of the fuel during the liner compression. We estimate the fuel loss by assuming that a rarefaction wave propagates into the fuel from the open end during the compression. There exists a self-similar solution[23] for such a rarefaction penetrating into a medium from the surface. The wave front penetrates a distance $\mathrm{X}=c_s t$, where c_s is the speed of sound in the medium ahead of the front. The position of each expanding gas element is related to their initial Lagrangian position ξ, by the expression $\xi=1+(x/\mathrm{X}-1)/4$. The density is given by $\rho=\rho_0\xi^3$. The mass that has expanded out of the surface boundary is found from the integral $M_L=\rho_0 A\int_{-3\mathrm{X}}^{0}\xi^3 dx$. We take the derivative with respect to time to find the mass loss rate and divide by the area to obtain the mass flux lost $F_L=(3/4)^4\rho_0 c_s$. We use this last result to estimate the mass that escape through the open end of the liner as it compresses where we assume that we can use the time-dependent value of $c_s=8.96\times 10^6\ \theta^{1/2}$ cm/s for DT. The gas temperature is found by assuming adiabatic compression, i.e., $\theta=\theta_0(\rho/\rho_0)^{2/3}$ where $\gamma=5/3$ has been assumed. After some algebra we obtain differential equations for the fraction of the fuel mass remaining in the liner. The results are

$$\dot{m}=\frac{c_{so}}{L}\left(\frac{r_H}{r_0}\right)^2\left(\frac{r_0}{r}\right)^{8/3} m^{4/3} \quad r>r_H \tag{24}$$

$$\dot{m}=\frac{c_{so}}{L}\left(\frac{r_0}{r}\right)^{2/3} m^{4/3} \quad r<r_H, \tag{25}$$

where r_0 is the initial radius of the liner and r_H is the radius of the laser entrance hole. Lasnex simulation of the liner implosions indicate that the inner boundary of the liner is well approximated by the expression

$$r=r_0[1-(t/t_p)^{5/3}], \tag{26}$$

where $t_p=60$ ns. These equations can be integrated analytically and expressed in terms of hypergeometric functions. Results are plotted in Fig. 16 as dashed curves, where the initial preheat temperature was assumed to be 0.2 keV. A series of 2D Lasnex simulations with the liner forced to obey Eq. (26) was performed to check the accuracy of this analytic model. The result is plotted in Fig. 16 as the solid curve. These results verify what we intuitively expect, namely, that the fuel fraction remaining at stagnation is made larger by either increasing the length of the liner or decreasing the size of the laser entrance hole. It should be noted that it is possible to design the liner so that the laser entrance hole closes as the liner implodes. We plan to perform fully integrated simulations to self-consistently include fuel loss during the implosion.

Downloaded 18 Jan 2011 to 134.253.26.11. Redistribution subject to AIP license or copyright; see http://pop.aip.org/about/rights_and_permissions

V. LINER MAGNETIZATION

The initial applied magnetic field must be generated slowly enough so that the difference between the magnetic pressure outside and inside the liner is not large enough to crush the liner. The rising magnetic field within the liner produces a voltage given by $V=\int 2\pi r E d\theta = -\dot{\phi} = IR$, where the resistance of the liner to azimuthal current is given by $R=2\pi\eta/z\Delta r$, and where η is the resistivity of the liner material, z is the length of the liner and Δr is the liner thickness. The solenoidal magnetic field inside the liner produced by azimuthal current I in the liner is given by the expression $B_L=\mu_0 I/z$. The total field within the liner is the difference between this internal field and the field supplied by the external field coils. Combining these equations we obtain $\dot{B}_L + B_L/\tau = \dot{B}_x$, where $\tau=\mu_0 r\Delta r/2\eta = R/L$. If we assume that the external field has the form $B_x(t)=B_A \sin(\omega t)$ and solve the ordinary differential equation, we obtain the result $B_{\text{int}}(t) = B_{\max}\omega\tau/(1+\omega^2\tau^2)\{[\sin(\omega t)/\omega\tau]+\cos(\omega\tau)+e^{-x/\omega\tau}\}$ for the magnitude of the field inside of the liner. The condition that the difference between the outside and the inside magnetic pressure is less than the buckling strength of the liner is expressed by the formula $(B_x^2-B^2)/2\mu_0 < S_{\text{crush}}(\Delta r/r)$, where S_{crush} is the strength of the liner material. Combining these results, we obtain the condition $\omega=4S_{\text{crush}}\eta/B_A^2 r^2$. Assuming $B_A=30$ T, $\omega \sim 1.4\times 10^4$ s^{-1} for beryllium and 2.6×10^3 s^{-1} for aluminum. Note that the result is independent of the liner aspect ratio due to the balance between the diffusion rate and the liner strength. We are constructing a capacitor bank coil system with a rise time exceeding 1 ms to maintain versatility in the choice of the liner material.

The return magnetic flux from the coils magnetizing the liner will have to cross the magnetically insulated transmission line (MITL) that feeds current from the Z machine to the liner, see Fig. 1. Care must be taken to insure that these fringe fields do not cause a large loss of current across the MITL. This is not expected to be a major obstacle since we successfully solved the same problem for magnetically insulated ion diodes.[35] Furthermore, we have performed preliminary particle-in-cell simulations, which indicate that this field should not cause a power flow problem.

VI. CONCLUSIONS

We have presented both 1D scaling and 2D stability simulations indicating that liner implosions with magnetized and preheated fuel could be an interesting path toward economical fusion. The 1D simulations indicate that both magnetization and fuel preheat are necessary to obtain interesting fusion yields with modest convergence ratios on an existing pulsed-power accelerator such as the Z machine. These magnetized liners are expected to be robust to anomalous transport, because the Hall parameter within the fuel is modest. Our 2D simulations indicate that a liner implosion can be robust against the MRT instability if the liner walls are made thick enough, because the bubbles formed at the outside of the liner will only be accelerated at a fraction of the overall acceleration of the liner. Experiments and more highly resolved 2D and 3D simulations are needed to determine how thick the liners must be, but our preliminary 2D simulations suggest that initial aspect ratios of 5–10 may produce the optimum fusion yields. We have proposed laser preheating of the DT fuel and analytic and numerical simulations indicate that this should be energetically feasible with the Z-Beamlet laser. Considerable work remains to determine the potential of this concept. We plan to perform simulations integrating the laser heating with the liner implosion. Details of the laser heating of deuterium plasmas will be studied using Z-Beamlet. We have shown that the fusion yield is relatively insensitive to mixing of the liner material into the fuel when the liner material is beryllium, but we need to determine the degree of fuel-liner mix using model calculations and ultimately experiments. We are designing and building the magnetic field coils and the capacitor bank needed to magnetize the fuel. We hope to accomplish these tasks soon and perform integrated experiments of this concept.

ACKNOWLEDGMENTS

Sandia is a multiprogram laboratory operated by Sandia Corporation, a Lockheed Martin Company, for the National Nuclear Security Administration of the United States Department of Energy under Contract No. DE-AC04-94AL85000.

[1] R. B. Spielman, C. Deeney, G. A. Chandler, M. R. Douglas, D. L. Fehl, M. K. Matzen, D. H. McDaniel, T. J. Nash, J. L. Porter, T. W. L. Sanford, J. F. Seamen, W. A. Stygar, K. W. Struve, S. P. Breeze, J. S. McGurn, J. A. Torres, D. M. Zagar, T. L. Gilliland, D. O. Jobe, J. L. McKenney, R. C. Mock, M. Vargas, T. Wagoner, and D. L. Peterson, Phys. Plasmas **5**, 2105 (1998).
[2] R. A. Vesey, M. C. Herrmann, R. W. Lemke, M. P. Desjarlais, M. E. Cuneo, W. A. Stygar, G. R. Bennett, R. B. Campbell, P. J. Christenson, T. A. Mehlhorn, and S. A. Slutz, Phys. Plasmas **14**, 056302 (2007).
[3] R. Landshoff, Phys. Rev. **76**, 904 (1949).
[4] J. Nuckolls, L. Wood, A. Thiessen, and G. Zimmerman, Nature (London) **239**, 139 (1972).
[5] M. M. Widner, 1980 (personal communication).
[6] M. M. Widner, C. J. Chang, A. V. Farnsworth, Jr., R. J. Leeper, T. S. Prevender, L. Baker, and J. N. Olsen, Bull. Am. Phys. Soc. **22**, 1139 (1977).
[7] M. A. Sweeney and A. V. Farnsworth, Jr., Nucl. Fusion **21**, 41 (1981).
[8] I. R. Lindemuth and R. C. Kirkpatrick, Nucl. Fusion **23**, 263 (1983).
[9] R. C. Kirkpatrick, I. R. Lindemuth, and M. S. Ward, Nucl. Fusion **27**, 201 (1994).
[10] R. E. Siemon, I. R. Lindemuth, and K. F. Schoenberg, Comments Plasma Phys. Controlled Fusion **18**, 363 (1999).
[11] R. D. Jones and W. C. Mead, Nucl. Fusion **26**, 127 (1986).
[12] T. A. Mehlhorn, B. B. Cipiti, C. L. Olson, and G. E. Rochau, Fusion Eng. Des. **83**, 948 (2008).
[13] D. C. Barnes, Comments Plasma Phys. Controlled Fusion **18**, 71 (1997).
[14] Y. B. Khariton, Usp. Fiziol. Nauk **120**, 706 (1976) [Sov. Phys. Usp. **19**, 1032 (1976)].
[15] I. R. Lindemuth, E. E. Reinovsky, R. E. Chrien, J. M. Christian, C. A. Ekdahl, J. H. Goforth, R. C. Haight, G. Idzorek, N. S. King, R. C. Kirkpatrick, R. E. Larson, G. L. Morgan, B. W. Olinger, H. Oona, R. T. Sheehey, J. S. Shlachter, R. C. Smith, L. R. Veeser, B. J. Warthen, S. M. Younger, V. K. Chernyshev, V. N. Mokhov, A. N. Demin, Y. N. Dolin, S. F. Garanin, V. A. Ivanov, V. P. Korchagin, O. D. Mikhailov, I. V. Morozov, S. V. Pak, E. S. Pavlovskii, N. Y. Seleznev, A. N. Skobelev, G. I. Volkov, and V. A. Yakubov, Phys. Rev. Lett. **75**, 1953 (1995).
[16] K. F. Schoenberg and R. E. Siemon, "Magnetized target fusion, a proof of principle research proposal," Report No. LA-UR-98-2413, 1998.
[17] M. Tuszewski, Nucl. Fusion **28**, 2033 (1988).
[18] T. Intrator, M. Taccetti, D. A. Clark, J. H. Degnan, D. Gale, S. Coffey, J. Garcia, P. Rodriguez, W. Sommars, B. Marshall, F. Wysocki, R. Siemon, R. Faehl, K. Forman, R. Bartlett, T. Cavazos, R. J. Faehl, M. H. Frese, D. Fulton, J. C. Gueits, T. W. Hussey, R. Kirkpatrick, G. F. Kiuttu, F. M.

Downloaded 18 Jan 2011 to 134.253.26.11. Redistribution subject to AIP license or copyright; see http://pop.aip.org/about/rights_and_permissions

Lehr, J. D. Letterio, I. Lindemuth, W. McCullough, R. Moses, R. E. Peterkin, R. E. Reinovsky, N. F. Roderick, E. L. Ruden, K. F. Schoenberg, D. Scudder, J. Shlachter, and G. A. Wurden, Nucl. Fusion **42**, 211 (2002).
[19]T. Intrator, S. Y. Zhang, J. H. Degnan, I. Furno, C. Grabowski, S. C. Hsu, E. L. Ruden, P. G. Sanchez, J. M. Taccetti, M. Tuszewski, W. J. Waganaar, and G. A. Wurden, Phys. Plasmas **11**, 2580 (2004).
[20]A. J. Kemp, M. Basko, and J. Meyer-ter-Vehn, Nucl. Instrum. Methods Phys. Res. A **464**, 192 (2001).
[21]O. V. Gotchev, N. W. Jang, J. P. Knauer, M. D. Barbero, R. Betti, C. K. Li, and R. D. Petrasso, J. Fusion Energy **27**, 25 (2008).
[22]D. D. Ryutov, Fusion Sci. Technol. **56**, 1489 (2009).
[23]Y. B. Zel'dovich and Y. P. Raizer, *Physics of Shock Waves and High-Temperature Hydrodynamic Phenomena* (Academic, New York, 1966), pp. 45–52.
[24]G. B. Whitham, *Linear and Nonlinear Waves* (Wiley, New York, 1974), p. 198.
[25]J. Lindl, Phys. Plasmas **2**, 3933 (1995).
[26]S. A. Slutz, M. R. Douglas, J. S. Lash, R. A. Vesey, G. A. Chandler, T. J. Nash, and M. S. Derzon, Phys. Plasmas **8**, 1673 (2001).
[27]A. R. Miles, Phys. Plasmas **16**, 032702 (2009).
[28]J. D. Lindl, P. Amendt, R. L. Berger, S. G. Glendinning, S. H. Glenzer, S. W. Haan, R. L. Kauffman, O. L. Landen, and L. J. Suter, Phys. Plasmas **11**, 339 (2004).
[29]S. I. Braginskii, *Reviews of Plasma Physics* (Consultants Bureau, New York, 1965), Vol. 1, p. 205.
[30]S. Atzeni and J. Meyer-Ter-Vehn, *The Physics of Inertial Fusion* (Clarendon, Oxford, 2004).
[31]R. M. White, D. A. Resler, and G. M. Hale, "FENDL/C-2.0. Charged-particle reaction data library for fusion applications," summary documentation by A. B. Pashchenko and H. Wienke, IAEA Report No. IAEA-NDS-177, 1997.
[32]M. M. Basko, A. J. Kemp, and J. Meyer-ter-Vehn, Nucl. Fusion **40**, 59 (2000).
[33]D. Ryutov, Phys. Plasmas **9**, 4085 (2002).
[34]G. B. Zimmerman and W. B. Kruer, Comments Plasma Phys. Controlled Fusion **2**, 51 (1975).
[35]S. A. Slutz, D. B. Seidel, and R. S. Coats, J. Appl. Phys. **59**, 11 (1986).

Downloaded 18 Jan 2011 to 134.253.26.11. Redistribution subject to AIP license or copyright; see http://pop.aip.org/about/rights_and_permissions